CHEMISTRY
A EUROPEAN JOURNAL

DOI: 10.1002/chem.200501101

The Characterisation of Molecular Alkali-Metal Azides

J. Steven Ogden,*[a] John M. Dyke,[a] William Levason,[a] Francesco Ferrante,[b] and Laura Gagliardi[b]

Abstract: Matrix isolation infrared (IR) studies have been carried out on the vaporisation of the alkali-metal azides MN_3 (M = Na, K, Rb and Cs). The results show that under high vacuum conditions, molecular KN_3, RbN_3 and CsN_3 are present as stable high-temperature vapour species, together with variable amounts of nitrogen gas and the corresponding metal atoms. The characterisation of these molecular azides is supported by ab initio molecular orbital calculations and density functional theory (DFT) calculations, and for CsN_3 in particular, by the detection of the isotopomers $Cs(^{14}N^{15}N^{14}N)$ and $Cs(^{15}N^{14}N^{14}N)$. The IR spectra are assigned to a "side-on" (C_{2v}) structure by comparison with the spectral features predicted both by vibrational analysis and calculation. The most intense IR features for KN_3, RbN_3 and CsN_3 isolated in nitrogen matrices lie at 2005, 2004.4 and 2002.2 cm^{-1}, respectively, and correspond to the N_3 asymmetric stretch. The N_3 bending mode in CsN_3 is identified at 629 cm^{-1}. An additional feature routinely observed in these experiments occurred at approximately 2323 cm^{-1} and is assigned to molecular N_2, perturbed by the close proximity of an alkali-metal atom. The position of this band appeared to show very little cation dependence, but its intensity correlated with the extent of sample thermal decomposition.

Keywords: alkali metals · azides · IR spectroscopy · matrix isolation · theoretical calculations

Introduction

There is considerable current interest in the preparation and characterisation of polynuclear nitrogen compounds, not least because of the potential role which they may play in energy storage. These studies range from electronic-structure calculations on pure nitrogen cluster species,[1–4] to the characterisation of a range of polynuclear cations,[5] or novel azide complexes.[6,7] The starting point for many of the experimental studies is a simple binary azide, and examples of these occur as well-established metal salts, such as MN_3 (M = alkali metal, Ag), and $M'(N_3)_2$ (M′ = Ba, Pb) or as essentially discrete molecular species such as HN_3 or ClN_3. The chemistry of such covalent azides has been extensively reviewed by Klapötke et al.[8–11]

We have been interested for many years in the formation and characterisation of the *molecular* salts produced by the vaporisation of the parent solids using matrix isolation infrared (IR) spectroscopy as the principal investigative tool.[12] In this context it is interesting to explore whether molecular alkali-metal azides can exist as stable chemical species, and whether they could be employed as synthetic reagents to produce higher nitrogen clusters.

The thermal decomposition of alkali-metal azides is a well-established route to the formation of the pure metal,[13] but CsN_3 nevertheless has sufficient thermal stability to be stable at least up to its melting point of approximately 580 K. The experiments described here were designed to explore the possibility that *molecular* alkali-metal azides might exist in the vapour phase, and subsequently to establish the shape of any such new species by IR matrix-isolation experiments supported by electronic-structure calculations. In the longer term, it may be envisaged that these novel molecular species might provide a new route to polynuclear nitrogen compounds. This combination of matrix-isolation experiments and electronic-structure calculations has recently been used by us to characterise a number of organic azide species and to study their decomposition mechanisms on pyrolysis.[14]

[a] Dr. J. S. Ogden, Prof. J. M. Dyke, Prof. W. Levason
School of Chemistry
University of Southampton
Southampton SO17 1BJ (UK)
Fax: (+44) 23-8059-3781
E-mail: j.s.ogden@soton.ac.uk

[b] Dr. F. Ferrante, Dr. L. Gagliardi
Department of Physical Chemistry
University of Palermo
90128 Palermo (Italy)

Experimental Section

Samples of the crystalline solids NaN_3 (99.99%) and CsN_3 (99.99%) were obtained from Aldrich and were used as received. LiN_3 was made from a metathesis reaction of Li_2SO_4 and NaN_3 in aqueous ethanol according to the literature,[15] and the crude LiN_3 was purified by two recrystallisations from hot absolute ethanol to remove small amounts of the sodium impurity. KN_3 was made from *n*-butyl nitrite and hydrazine in alcoholic KOH solution by the method of Miller and Audrieth.[16] The crude product was purified by dissolution in the minimum volume of cold water and reprecipitated with ethanol. RbN_3 was made by the same method,[16] using RbOH.

The general features of our matrix isolation and IR analysis equipment have been described elsewhere.[17] The studies described here involve the vaporisation under vacuum of the solid azides from silica sample holders heated externally by a small resistance furnace. In general, azides have the potential to detonate on heating, and safety precautions to mitigate this were routinely put in place. However, no explosions were encountered during the course of these studies.

In a typical experiment, the solid azide sample (ca. 300 mg) was heated stepwise to a maximum temperature of approximately 800 K, and the vapour-phase products co-condensed with a large excess ($>\times1000$) of matrix gas (Ar or N_2, purities $>99.999\%$) onto a CsI window cooled to approximately 10–12 K. Deposition times at any particular temperature were typically 30 min, and IR spectra were recorded after each deposition.

Isotopic data (^{15}N) were obtained from samples in natural abundance and isotopic effects modelled both by a traditional vibrational analysis (GF matrix method) and by the electronic-structure calculations described below.

Computational methods: All electronic-structure calculations were carried out at the density functional theory (DFT) and second-order Möller–Plesset perturbation theory (MP2) levels. In the DFT approach, the three-parameter hybrid functional B3LYP,[18] mixing Becke's exchange with the nonlocal correlation functional provided by Lee, Parr and Yang, was used. The basis sets selected were as follows: For nitrogen atoms, an augmented correlation-consistent basis set (aug-cc-pvtz[19]) was used in all calculations; this is a triple-zeta-valence basis set which comprises polarisation and diffuse functions. For sodium atoms, the corresponding basis set cc-pvtz,[20] without diffuse functions, was employed whereas for the heavier atoms, potassium, rubidium and caesium, a relativistic effective core potential (RECP) proved to be the best choice. The RECP was the Stuttgart relativistic small core ECP (RSC 1997 ECP[21]): it is a small-core quality ECP described by s-, p-, d-, f- and g-type functions; it takes into account the 10, 28 and 46 core electrons for potassium, rubidium and caesium, respectively. A valence basis set with the (7s6p)/[5s4p] contraction scheme[22] was used for the remaining 9 outer-shell electrons of K, Rb and Cs. The molecular structures of all the alkaline-metal azides were optimised by checking the Hessian matrix; the vibrational frequencies and the zero-point energy were estimated by using the harmonic approximation. All calculations were performed by using the Gaussian 03 package.[23]

At the optimized B3LYP geometries, single-point energy calculations were also performed by using the complete active space (CAS) SCF method[24] to generate molecular orbitals and reference functions for subsequent multiconfigurational second-order perturbation calculations of the dynamic correlation energy (CASPT2).[25] The quantum chemical calculations were performed using the software MOLCAS6.2.[26]

The active space choice is crucial for the method. Calculations with several active spaces were performed, including a linear combination of the nitrogen 2p orbitals and the caesium orbitals of appropriate symmetry. The largest calculation comprised 10 active electrons in 11 active orbitals.

The Stuttgart effective core potentials were used for the Cs atom.[27] The accompanying basis set for the 9 valence electrons was contracted to 5s4p. For the N atom, a basis set of atomic natural orbital (ANO) type, available in the MOLCAS6.2 library, was used. A primitive set of 10s6p3d was contracted to 3s2p1d.

Results and Discussion

Vaporisation of solid CsN_3: Figure 1a shows part of a typical nitrogen matrix IR spectrum obtained after the heating of anhydrous CsN_3 at 440 K. At this temperature, there is no evidence of any sublimation, and the only feature present in

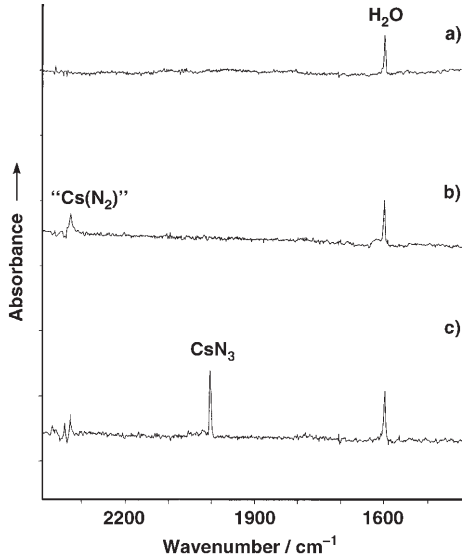

Figure 1. Nitrogen matrix IR spectra obtained at various stages in the vaporisation of caesium azide: a) after heating at approximately 440 K; b) after heating at approximately 670 K; c) after heating at approximately 750 K.

this spectrum is the intense bending mode of (nonrotating) matrix-isolated H_2O at approximately 1597 cm^{-1}. This band is believed to arise from the desorption of small amounts of water from the silica walls of the deposition system. The other two fundamentals of H_2O were also present in the extended (4000–400 cm^{-1}) spectrum.

At a temperature of approximately 670 K, a khaki-bronze film of metallic caesium could be observed on the off-axis walls of the deposition system, and a small pressure rise of approximately 2×10^{-6} mbar was also typically observed at this stage. Figure 1b shows a typical spectrum obtained at this temperature. In addition to the H_2O band at 1597 cm^{-1}, a further new band is present at 2323 cm^{-1}, and numerous experiments confirmed that this band was always associated with the appearance of the metallic deposit. At this stage it would appear that the CsN_3 is at least partially decomposing into $Cs+N_2$.

On further increasing the temperature to approximately 750 K, the molten CsN_3 was observed to "boil", and simultaneously to produce a white sublimate on the cooler parts of the vaporisation tube. The IR spectrum obtained at this stage in the experiment shows the 1597 cm^{-1} H_2O band, a weaker 2323 cm^{-1} band, and a prominent new band at 2002.2 cm^{-1}. A typical spectrum is shown in Figure 1c.

Further heating of the molten CsN_3 resulted ultimately in the vaporisation of the whole sample, *without apparent de-*

composition into metallic caesium, and subsequent IR analysis of the white sublimate (after removal under an inert atmosphere at room temperature) showed it to be crystalline CsN_3. The spectra obtained from such prolonged depositions also revealed a number of additional sharp bands, notably, very weak features at 629 and 970 cm^{-1}, together with a broader band at approximately 2017 cm^{-1}, and a doublet at 2149/2139 cm^{-1}. Three of these features can be identified in Figure 2, which shows a survey spectrum obtained after extensive deposition at approximately 760 K.

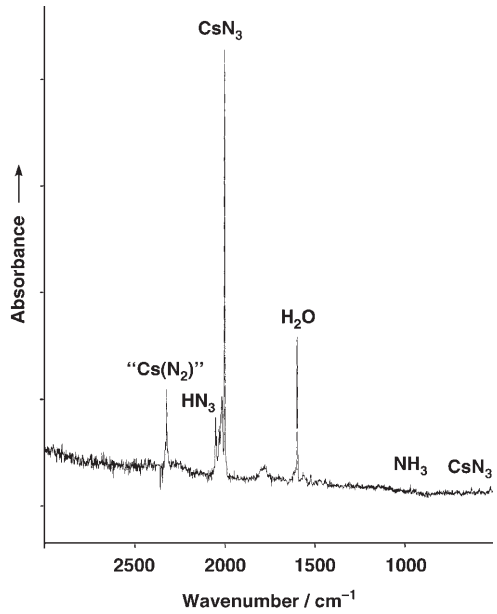

Figure 2. Nitrogen matrix IR spectrum (3000–500 cm^{-1}) obtained from prolonged vaporisation of CsN_3 at approximately 760 K.

A number of experiments were also carried out using argon as the matrix material. These also gave sharp bands, but the spectra were of varying complexity. In the early stages of sublimation, the bands at approximately 2323 and 2002.2 cm^{-1} were both observed, but continued deposition led first to the appearance of weaker, broad features in the range 1990–2000 cm^{-1}, but ultimately to a sharper, intense feature at 1987.6 cm^{-1}.

This behaviour is consistent with the partial decomposition of solid CsN_3 into $Cs+N_2$, which produces a mixed argon/nitrogen environment for any species vaporising at this stage. At higher temperatures, however, vaporisation appears to take place congruently, and the spectrum then reflects a pure(r) argon matrix environment for which a shift of approximately 14.6 cm^{-1} in the position of the most intense band is apparent, relative to nitrogen. Because of this complication, the majority of experiments were carried out using nitrogen as the matrix host. The initial conclusion from these experiments, therefore, is that CsN_3 may be sublimed at least partially *without* decomposition under high vacuum conditions, and that Figure 2 contains spectral features due to molecular CsN_3.

The IR spectra of the solid alkali-metal azides are well documented, and typically show an intense antisymmetric stretch in the region 2000–2100 cm^{-1}, and a very much weaker bend at approximately 620–650 cm^{-1}. The symmetric stretch is generally not observed (it would be infrared inactive in the free anion), but has been reported at approximately 1340–1350 cm^{-1} from Raman studies. By analogy with the many alkali-metal salt molecules for which vibrational data are now available, the IR spectrum of molecular CsN_3 would be expected to be broadly very similar to that of the free N_3^- ion. Figure 2 shows a typical nitrogen-matrix spectrum obtained from CsN_3 over a wider spectral range. The band at 2002.2 cm^{-1} and a very weak feature at 629 cm^{-1} are both provisionally assigned to *molecular* CsN_3 by comparison with the data from the solid phase. Despite a detailed search, no features were observed in the spectral region expected for the symmetric stretch (1250–1400 cm^{-1}).

The weak features at 970 cm^{-1} and 2149/2139 cm^{-1} are assigned to the most intense fundamentals of NH_3 and HN_3, respectively. These species are tentatively believed to arise from reaction between molecular CsN_3 and H_2O during co-condensation.

If the assignment of the intense 2002.2 cm^{-1} band to CsN_3 is correct, one might anticipate a small but significant shift in its position when caesium is replaced by a different alkali metal, as a result of interaction between the N_3 group and the coordinated cation.

Vaporisation of NaN_3, KN_3 and RbN_3: Several analogous experiments were carried out in which these alkali-metal azides were vaporised. The products were isolated in nitrogen matrices, and the spectral region 2400–1900 cm^{-1} was examined closely for any features that might correspond to the intense 2002.2 cm^{-1} band in the caesium system. In many cases, some decomposition was observed to take place at approximately 570 K, prior to melting, as indicated by the formation of reflecting films of sublimed metal, and a feature at approximately 2323 cm^{-1} was typically observed at this stage. On further heating, no new bands near 2000 cm^{-1} were ever observed from NaN_3, but KN_3 and RbN_3 subsequently melted, and at a temperature of approximately 750 K gave new features at 2005.0 and 2004.4 cm^{-1}, respectively. Figure 3 compares the positions (and widths) of these bands with the principal CsN_3 feature, and it is evident that these small shifts support the predicted cation dependency for a molecular MN_3 species. However, unlike the caesium system, it proved impossible to build up sufficient intensity in these K and Rb features to observe the corresponding bending or ^{15}N features, because their growth was always accompanied by extensive sample decomposition.

^{15}N isotopic features: Figure 2 shows that although the intense CsN_3 absorption at 2002.2 cm^{-1} has extraneous weaker features at higher frequency, there are few, if any such features in the region 2000–1900 cm^{-1}, where the weak bands arising from ^{15}N isotopomers in natural abundance are expected to occur. The observation of these fundamentals can

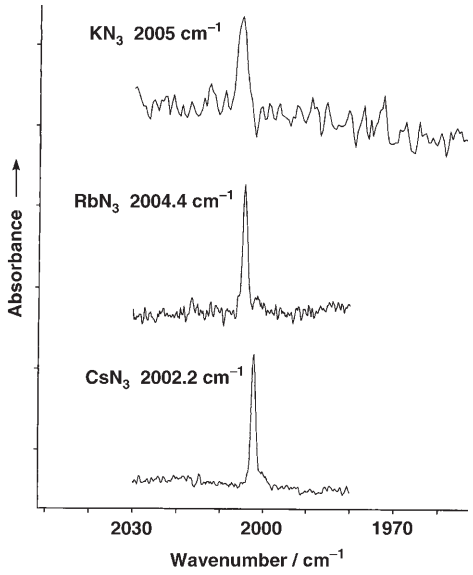

Figure 3. Nitrogen matrix IR spectra obtained from KN_3, RbN_3 and CsN_3 in the spectral region 2030–1980 cm^{-1}.

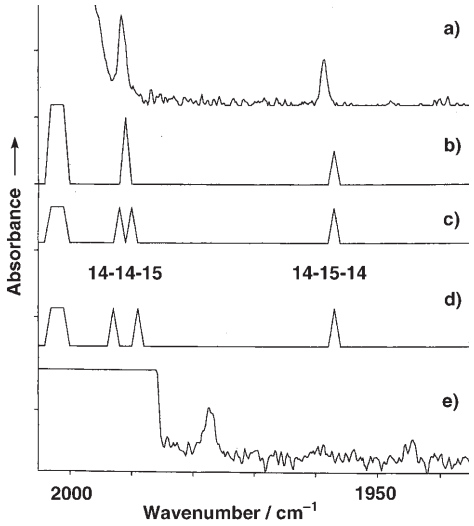

Figure 4. Observed and calculated ^{15}N isotopic effects for matrix-isolated CsN_3: a) ^{15}N isotopic features observed in a nitrogen matrix; b) ^{15}N isotopic features calculated for side-on (C_{2v}) bonding using the parameters of calculation I (Table 1); c) and d) calculated ^{15}N isotopic features using the parameters of calculations III and IV, respectively, for end-on bonding; e) ^{15}N isotopic features observed in an argon matrix.

provide evidence for the shape of molecular CsN_3, in addition to confirming its identification. Several experiments were carried out in which this spectral region was studied in detail.

The argon-matrix data for CsN_3 was in general complicated by the effects of the mixed Ar/N_2 matrix, but fortunately, the corresponding spectral region to low frequency of the "pure argon matrix" band at 1987.6 cm^{-1} was similarly free of extraneous features. Satisfactory argon-matrix spectra could therefore also be obtained for the ^{15}N isotopic species.

Figure 4a shows the spectral region 2010–1950 cm^{-1} obtained for CsN_3 in a nitrogen matrix. The very intense band centred near 2000 cm^{-1} is the 2002.2 cm^{-1} fundamental of the most isotopically abundant species, $Cs^{14}N_3$, but in addition, two weak features can be identified at 1991.8 and 1958.7 cm^{-1}, shifted by 10.4 and 43.5 cm^{-1}, respectively, from the main band. In an argon matrix, the main isotopomer band lies at 1987.6 cm^{-1}, and corresponding weak features were noted at 1977.5 and 1944.5 cm^{-1}. The natural abundance of ^{15}N is approximately 0.36%, and these weak features are provisionally assigned to the isotopic variants $Cs(^{15}N^{14}N^{14}N)$ and $Cs(^{14}N^{15}N^{14}N)$.

Normal coordinate analysis (NCA) modelling of isotopic features: The most convenient starting point for NCA modelling of the assigned isotopic features is the establishment of suitable force fields for the free (linear) azide ion that reproduce the intense feature assigned to the antisymmetric stretch at approximately 2000 cm^{-1}. For this simple system, there are only two potential constants to be considered: the principal N–N stretch, denoted F_R, and the interaction constant F_{RR}. In the simple-harmonic approximation, both these can be evaluated precisely if the positions of both the symmetric ($\tilde{\nu}_1$) and antisymmetric ($\tilde{\nu}_3$) stretching frequencies are known. The positions of these modes in a truly isolated azide ion are unknown, but in solid KN_3 they have been reported at 1344 and 2041 cm^{-1}, respectively, from a combination of IR and Raman studies.[28,29]

Assuming for the moment that in matrix-isolated CsN_3 the anion is effectively "free", a value for $\tilde{\nu}_3$ can be taken as the observed nitrogen-matrix feature at 2002.2 cm^{-1}. However, as $\tilde{\nu}_1$ is not known, a range of values must be tried that lead to a range of solutions for F_R and F_{RR}, all of which reproduce the observed value for $\tilde{\nu}_3$. For each pair of values, F_R and F_{RR}, it is then straightforward to calculate the expected positions of all isotopic $^{14}N/^{15}N$ combinations for the isolated azide ion. This procedure must produce identical values of ν_3 for all pairs of F_R and F_{RR} for a particular "symmetrical" isotopomer, such as 15-15-15, 14-15-14 and 15-14-15, because the isotope shifts relative to the parent 14-14-14 species are determined solely by the Product Rule. For the less-symmetrical species, 14-14-15 and 14-15-15, the positions of $\tilde{\nu}_3$ will in principle depend on the particular values of F_R and F_{RR}, because for these molecules there is coupling between $\tilde{\nu}_1$ and $\tilde{\nu}_3$. In practice, however, this coupling is very small. Even when the notional position of $\tilde{\nu}_1$ is varied from 1200 to 1400 cm^{-1}, it turns out that the positions of all the isotopic frequencies associated with $\tilde{\nu}_3$ are constant to within 0.2 cm^{-1}.

This result removes any concern that there may be about the true position of $\tilde{\nu}_1$, and the effect that this may have on the subsequent interpretation of isotope patterns in the $\tilde{\nu}_3$ region. The next stage is to model the isotopic shifts expected for the side-on and end-on structures of CsN_3.

For the side-on (C_{2v}) structure, we assume initially that the N_3 unit is still essentially linear, and that although $\tilde{\nu}_3$ can in principle couple with the low frequency cation motion, it is essentially decoupled. However, the distinguishing feature

of this structure is that there is no linkage isomerisation associated with cation coordination, and there is only one distinct isotopomer containing the 14-14-15 group. Furthermore, this isotopomer occurs at twice the abundance of the more symmetrical 14-15-14 variant. The isotopic features expected for side-on bonding are therefore almost independent of uncertainties in the force field, and for a wide range of parameters F_R and F_{RR} this modelling predicts positions of 1957.2 and 1991.3 cm^{-1} for the two most abundant isotopomers 14-15-14 and 14-14-15, respectively, relative to the parent 14-14-14 band at 2002.2 cm^{-1}. The model also predicts an intensity ratio of 2:1 for the 1991.3 and 1957.2 cm^{-1} bands from their relative abundances. Isotope shift calculations were also carried out for C_{2v} structures in which the N-N-N bond angle was varied over the range 170–180°. These showed that this slight departure from linearity produced essentially no change in the predicted positions of the ^{15}N isotopomers.

For the end-on structure, the effect on the vibrations of the N_3 unit can be visualised as being represented by two distinct principal force constants, denoted $F_{R'}$ and $F_{R''}$. This distinction reflects the fact that Cs coordinates to one end of the N_3 ion, which results in the existence of two distinct isomers for unsymmetrical substitution: Cs-14-14-15 and Cs-15-14-14. The effect of this on the IR spectrum will in principle be to split the "14-14-15" isotope feature, with the magnitude of the splitting being determined by the difference between $F_{R'}$ and $F_{R''}$. This effect can also be modelled, and the isotopic band position can be calculated for sets of values for $F_{R'}$, $F_{R''}$ and F_{RR}, all of which generate the parent 14-14-14 band at 2002.2 cm^{-1}. The main point of interest here is to discover to what extent $F_{R'}$ and $F_{R''}$ must differ for the effect to be detected as a distinct splitting of the "14-14-15" isotopic feature. Experimentally, this band (at 1991.8 cm^{-1} in a nitrogen matrix) is essentially *the same width* (see Figure 4a) as the unsplittable 14-15-14 feature at 1958.7 cm^{-1}. It is considered very unlikely that this result would be compatible with the end-on model. Calculations show that it would require the difference between $F_{R'}$ and $F_{R''}$ to be less than approximately 1% for the splitting not to be at least partially resolved.

Table 1 summarises the results of this modelling for the observed CsN_3 isotopic data in a nitrogen matrix. The agreement between observed and calculated band positions fully confirms their assignment as N_3 ($\tilde{\nu}_3$) modes. Figure 4b–d shows pictorially how typical calculations for side-on and end-on coordination compare with the experimentally observed nitrogen matrix ^{15}N spectra. The most significant feature is the approximate 2:1 intensity ratio for the bands at 1991.8 and 1958.7 cm^{-1}, as predicted for the side-on C_{2v} structure (Figure 4b, calculation I). The small differences between observed and calculated band positions are attributed to the neglect of anharmonicity. Figure 4c and d reproduce the band positions generated by calculations III and IV, and show, in contrast, the doublet splittings predicted with two different force fields for the linear model.

Table 1. Observed and calculated (NCA) vibration frequencies [cm^{-1}] for isotopic CsN_3 species in nitrogen matrices.[a]

Observed[b]	Calculated (I)	Calculated (II)	Assignment[c]
2002.2	2002.2	2002.2	14-14-14
1991.8	1991.25	1991.3	14-14-15
1958.7	1957.2	1957.2	14-15-14
	Calculated (III)	Calculated (IV)	Assignment[d]
	2002.2	2002.2	Cs-14-14-14
	1992.1	1993.3	Cs-14-14-15
	1990.4	1989.1	Cs-15-14-14
	1957.2	1957.2	Cs-14-15-14

[a] Force constant parameters used in the calculations are as follows: for I: $F_R = 11.444$, $F_{RR} = 0.427$ mdyne A^{-1} (gives parent $\tilde{\nu}_1 = 1200\ cm^{-1}$); for II: $F_R = 12.474$, $F_{RR} = 1.458$ mdyne A^{-1} (gives parent $\tilde{\nu}_1 = 1300\ cm^{-1}$); for III: $F_{R'} = 11.182$, $F_{R''} = 11.711$, $F_{RR} = 0.434$ mdyne A^{-1}; for IV: $F_{R'} = 10.800$ $F_{R''} = 12.130$, $F_{RR} = 0.470$ mdyne A^{-1}. [b] Frequency accuracy 0.5 cm^{-1}. [c] Antisymmetric stretch: C_{2v} structure; side-on coordination by Cs. [d] Antisymmetric stretch: linear structure; end-on coordination.

The fifth spectrum displayed here (Figure 4e) shows the analogous ^{15}N features observed in an argon matrix, where again, there is no evidence for a linkage isomer splitting, and the 2:1 intensity ratio is evident.

Search for N_3 symmetric stretch: As indicated above, no spectroscopic features were observed that could be attributed to the (technically IR-active) symmetric stretch. For this reason, the NCA was based upon an essentially linear N-N-N unit. However, the electronic-structure calculations (see below) indicate a small departure from linearity of approximately 6° for the C_{2v} CsN_3 molecule, and it is of some interest to explore whether one might expect to observe the symmetric N_3 stretch for this degree of nonlinearity. Using the bond dipole model, within the Wilson GF approach,[30] it may be shown that if I_3 and I_1 denote the intensities of the antisymmetric and symmetric stretches, respectively, then Equation (1) is valid for a C_{2v}-symmetric triatomic XY_2 molecule:

$$\frac{I_3}{I_1} = \frac{\tan^2\theta(M_X + 2M_Y\sin^2\theta)}{(M_X + 2M_Y\cos^2\theta)} \quad (1)$$

in which the YXY bond angle is 2θ, and M_X and M_Y are the atomic masses of X and Y, respectively. This approach has been shown to have value in the estimation of bond angles in other matrix-isolated species.[31] Setting $M_X = M_Y = 14$, and $\theta = 87°$ gives a ratio of approximately 1090:1 for the intensity ratio I_3/I_1. The failure to definitely locate the symmetric stretch in this work is therefore not entirely unexpected.

Electronic-structure calculations on molecular alkali-metal azides: Two minimum-energy structures were located for molecular alkali-metal azides at the B3LYP and MP2 levels: the end-on linear structure (**I**) and the side-on (C_{2v}) structure (**II**), as shown below.

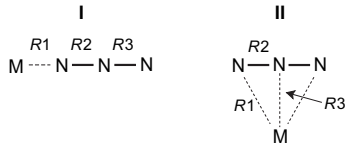

The results of these calculations as regards molecular structure were clear-cut for LiN_3, NaN_3, RbN_3 and CsN_3. The lowest-energy configurations for both RbN_3 and CsN_3 were predicted to be side-on by both methods, whereas LiN_3 and NaN_3 were predicted to have a linear geometry by both methods. In the case of KN_3, the B3LYP calculations predicted a linear geometry, but the MP2 method indicated side-on bonding. For LiN_3, NaN_3, KN_3, RbN_3 and CsN_3, the relative energies (C_{2v}–linear) at the B3LYP level are +0.44, +0.20, +0.01, −0.02 and −0.01 eV, respectively, and +0.25, +0.05, −0.10, −0.12 and −0.11 eV, respectively, at the MP2 level. These calculations also indicated that the angles N-N-N for the C_{2v} geometries were all in the range 169–175°, and that for CsN_3 in particular, this angle (internal to the ring) is predicted to be approximately 174°. The structural data is summarised in Table 2.

Subsequent calculations of the expected vibrational frequencies generally produced values for the N_3 antisymmetric stretch in CsN_3 that were somewhat higher than the experimental result (2002.2 cm^{-1}), with the closest prediction (2086 cm^{-1}) coming from the B3LYP calculation for the C_{2v} structure. The difference between these observed and calculated frequencies arises because of the neglect of anharmonicity in the calculation and only partial allowance for electron correlation. This calculation also satisfactorily reproduced the ^{15}N isotopic shifts, with a $\tilde{\nu}_3$ [(14-14-15)–(14-15-14)] separation of 35 cm^{-1} (B3LYP) compared with the experimental separation of 33 cm^{-1}. As indicated above, the degeneracy of the bending mode in the N_3 ion is lifted for side-on bonding, and this B3LYP calculation gave values of 663 and 687 cm^{-1} for the positions of the two components. The experimental data in this spectral region revealed only one (very weak) feature at 629 cm^{-1}, but the existence of a second distinct component could not be ruled out. Both types of calculation predict that the relative intensity of the symmetric N-N-N stretch for the C_{2v} structure is effectively zero compared with the antisymmetric stretch: a conclusion that confirms the previous estimate using the bond dipole model. Table 2 summarises the results obtained from the calculations on the linear and C_{2v} structures for CsN_3 at both the B3LYP and MP2 levels.

The CASSCF/CASPT2 calculations indicate that both structures have singlet closed-shell ground states, and that

Table 2. Calculated energies[a] and molecular parameters[a] for linear and C_{2v} structures of CsN_3.

	End-on (linear) coordination							
	B3LYP				MP2			
	14-14-14	15–14-14	14-15-14	14-14-15	14-14-14	15-14-14	14-15-14	14-14-15
geometry								
*R*1	2.682				2.627			
*R*2	1.193				1.210			
*R*3	1.155				1.187			
energy	−184.44656	−184.44666	−184.44674	−184.44666	−183.87354	−183.87364	−183.8737	−183.87363
IR frequencies and intensities								
Cs–N stretch	192 (75)	190 (74)	190 (73)	190 (73)	201 (76)	199 (75)	199 (75)	199 (75)
Cs-N-N bend[b]	55 (7)	53 (7)	55 (7)	54 (8)	89 (7)	87 (6)	89 (7)	88 (7)
N-N-N bend[b]	660 (6)	656 (6)	645 (6)	656 (6)	624 (3)	620 (2)	610 (3)	621 (2)
N-N-N stretch (s)	1387 (94)	1360 (94)	1387 (98)	1368 (85)	1249 (28)	1227 (27)	1249 (28)	1229 (27)
N-N-N stretch (as)	2148 (1313)	2141 (1279)	2100 (1267)	2131 (1306)	2155 (681)	2143 (659)	2106 (664)	2142 (675)

	Side-on (C_{2v}) coordination					
	B3LYP			MP2		
	14-14-14	15-14-14	14-15-14	14-14-14	15-14-14	14-15-14
geometry						
*R*1	3.053			2.977		
*R*2	1.178			1.206		
*R*3	2.876			2.786		
angle N-Cs-N	45.3			47.7		
angle N-N-N	174.5			173.8		
energy	−184.447076	−184.447179	−184.447256	−183.877586	−183.877682	−183.877764
IR frequencies and intensities						
Cs–N stretch (s)	178 (54)	177 (53)	177 (53)	191 (55)	189 (54)	190 (54)
Cs–N stretch (as)	114 (1)	112(1)	114(1)	140(2)	138(2)	140(2)
out of plane bend	663 (3)	660 (3)	649 (3)	606 (0)	603 (0)	593 (0)
in-plane bend	687 (1)	684 (1)	671 (2)	624 (0)	621 (0)	609 (0)
N-N-N stretch (s)	1360 (0)	1336 (0)	1359 (0)	1190 (0)	1170 (0)	1190 (0)
N-N-N stretch (as)	2086 (952)	2075 (938)	2040 (918)	2146 (301)	2135 (296)	2099 (293)

[a] Bond lengths (*R*) in Å. Angles in degrees. Energies in atomic units, IR frequencies in cm^{-1}, IR intensities (in parentheses) in km mol^{-1}. [b] Doubly degenerate.

the "side-on" structure lies about 6 kcal mol^{-1} lower in energy than the linear structure. This result therefore confirms the DFT results.

Conclusion

This work has conclusively demonstrated the existence of the stable *molecular* alkali azides KN_3, RbN_3 and CsN_3 produced as vapour species by heating the respective crystalline solids under vacuum conditions. When isolated in nitrogen matrices, these molecules are characterised by distinctive IR absorptions in the range 2000–2010 cm^{-1}, and for the caesium salt, the additional observations of ^{15}N isotopic features very strongly support a C_{2v} structure involving side-on cation coordination to the azide group. These experimental conclusions are also supported by electronic-structure calculations using both B3LYP and MP2 methods.

Acknowledgements

We gratefully acknowledge Qinetiq Ltd. (UK) for providing financial support for this work, which was carried out as part of the Weapons, Platforms and Effectors domain of the Ministry of Defence (MoD) research programme. The electronic-structure calculations were performed using the UK National Computational Software Service (EPSRC).

[1] M. T. Nguyen, *Coord. Chem. Rev.* **2003**, *244*, 93.
[2] M. T. Nguyen, T.-K. Ha, *Chem. Phys. Lett.* **2001**, *335*, 311.
[3] L. Gagliardi, S. Evangelisti, V. Barone, B. O. Roos, *Chem. Phys. Lett.* **2000**, *320*, 518.
[4] M. Straka, *Chem. Phys. Lett.* **2002**, *358*, 531.
[5] a) K. O. Christe, W. W. Wilson, J. A. Sheehy, J. A. Boatz, *Angew. Chem.* **1999**, *111*, 2112; *Angew. Chem. Int. Ed.* **1999**, *38*, 2004; b) D. A. Dixon, D. Feller, K. O. Christe, W. W. Wilson, A. Vij, V. Vij, H. D. B. Jenkins, R. M. Olson, M. S. Gordon, *J. Am. Chem. Soc.* **2004**, *126*, 834.
[6] a) R. Haiges, J. A. Boatz, S. Schneider, T. Schoer, M. Yousufuddi, K. O. Christe, *Angew. Chem.* **2004**, *116*, 3210; *Angew. Chem. Int. Ed.* **2004**, *43*, 3148; b) L. Gagliardi, P. Pyykko, *Inorg. Chem.* **2003**, *42*, 3074.
[7] a) R. Haiges, J. A. Boatz, A. Vij, M. Gerken, S. Schneider, T. Schoer, K. O Christe, *Angew. Chem.* **2003**, *115*, 6031; *Angew. Chem. Int. Ed.* **2003**, *42*, 5851; b) C. Knapp, J. Passmore, *Angew. Chem.* **2004**, *116*, 4938; *Angew. Chem. Int. Ed.* **2004**, *43*, 4834.
[8] I. C. Tornieporth-Oetting, T. M. Klapötke, *Angew. Chem.* **1995**, *107*, 559; *Angew. Chem. Int. Ed. Engl.* **1995**, *34*, 511.
[9] T. M. Klapötke, *Chem. Ber./Recl.* **1997**, *130*, 443.
[10] W. Fraenke, T. M. Klapötke, "Recent Developments in the Chemistry of Covalent Main Group Azides" in *Inorganic Chemistry Highlights* (Eds.: G. Meyer, D. Naumann, L. Wesemann), Wiley-VCH, Chichester, **2002**.
[11] I. C. Tornieporth-Oetting, T. M. Klapötke, "Covalent Inorganic Non-Metal Azides" in *Combustion Efficiency and Air Quality* (Eds.: I. Hargittai, T. Vidoczy), Plenum Press, New York, **1995**, p. 51.
[12] See, for example: a) I. R. Beattie, J. S. Ogden, D. D. Price, *J. Chem. Soc. Dalton Trans.* **1979**, 1460; b) T. N. Day, R. A. Gomme, J. S. Ogden, *J. Chem. Soc. Dalton Trans.* **1997**, 1957.
[13] See, for example: G. Brauer, *Handbook of Preparative Inorganic Chemistry, Vol. 1*, Academic Press, New York, **1963**, p. 959.
[14] See, for example: J. M. Dyke, G. Levita, A. Morris, J. S. Ogden, A. A. Dias, M. Algarra, J. P. Santos, M. L. Costa, P. Rodrigues, M. M. Andrade, M. T. Barros, *Chem. Eur. J.* **2005**, *11*, 1665.
[15] N. Hofmann-Bang, *Acta Chem. Scand.* **1957**, *11*, 581.
[16] M. W. Miller, L. F. Audrieth, *Inorg. Synth.* **1946**, *1*, 140.
[17] See, for example: A. K. Brisdon, R. A. Gomme, J. S. Ogden, *J. Phys. Chem.* **1991**, *95*, 2927.
[18] a) A. D. Becke, *J. Chem. Phys.* **1993**, *98*, 5648; b) P. J. Stephens, J. F. Devlin, C. F. Chabalowski, M. J. Frisch, *J. Phys. Chem.* **1994**, *98*, 11623.
[19] a) T. H. Dunning, Jr., *J. Chem. Phys.* **1989**, *90*, 1007; b) R. A. Kendall, T. H. Dunning, Jr., R. J. Harrison, *J. Chem. Phys.* **1992**, *96*, 6796.
[20] a) D. E. Woon, T. H. Dunning, Jr., *J. Chem. Phys.* **1993**, *98*, 1358; b) D. E. Woon, T. H. Dunning, Jr., *J. Chem. Phys.* **1995**, *103*, 4572.
[21] T. Leininger, A. Nicklass, W. Küchle, H. Stoll, M. Dolg, A. Bergner, *Chem. Phys. Lett.* **1996**, *255*, 274.
[22] Institut für Theoretische Chemie, Universität Stuttgart. ECPs and corresponding valence basis sets. http://www.theochem.uni-stuttgart.de/. The ECP for Rb and Cs are indicated as ECP28MWB and ECP46MWB, respectively.
[23] Gaussian 03, Revision B.05, M. J. Frisch, G. W. Trucks, H. B. Schlegel, G. E. Scuseria, M. A. Robb, J. R. Cheeseman, J. A. Montgomery, Jr., T. Vreven, K. N. Kudin, J. C. Burant, J. M. Millam, S. S. Iyengar, J. Tomasi, V. Barone, B. Mennucci, M. Cossi, G. Scalmani, N. Rega, G. A. Petersson, H. Nakatsuji, M. Hada, M. Ehara, K. Toyota, R. Fukuda, J. Hasegawa, M. Ishida, T. Nakajima, Y. Honda, O. Kitao, H. Nakai, M. Klene, X. Li, J. E. Knox, H. P. Hratchian, J. B. Cross, V. Bakken, C. Adamo, J. Jaramillo, R. Gomperts, R. E. Stratmann, O. Yazyev, A. J. Austin, R. Cammi, C. Pomelli, J. W. Ochterski, P. Y. Ayala, K. Morokuma, G. A. Voth, P. Salvador, J. J. Dannenberg, V. G. Zakrzewski, S. Dapprich, A. D. Daniels, M. C. Strain, O. Farkas, D. K. Malick, A. D. Rabuck, K. Raghavachari, J. B. Foresman, J. V. Ortiz, Q. Cui, A. G. Baboul, S. Clifford, J. Cioslowski, B. B. Stefanov, G. Liu, A. Liashenko, P. Piskorz, I. Komaromi, R. L. Martin, D. J. Fox, T. Keith, M. A. Al-Laham, C. Y. Peng, A. Nanayakkara, M. Challacombe, P. M. W. Gill, B. Johnson, W. Chen, M. W. Wong, C. Gonzalez, J. A. Pople, Gaussian, Inc., Wallingford CT, **2004**.
[24] B. O. Roos in *Advances in Chemical Physics: Ab Initio Methods in Quantum Chemistry-II* (Ed.: K. P. Lawley), Wiley, Chichester, **1987**, p. 399–445.
[25] K. Andersson, P.-Å. Malmqvist, B. O. Roos, A. J. Sadlej, K. J. Wolinski, *Phys. Chem.* **1990**, *94*, 5483.
[26] G. Karlstrom, R. Lindh, P.-Å. Malmqvist, B. O. Roos, U. Ryde, V. Veryazov, P. O. Widmark, M. Cossi, B. Schimmelpfennig, P. Neogrady, L. Seijo, *Comput. Mater. Sci.* **2003**, *28*, 222.
[27] P. Fuentealba, H. Stoll, L. von Szentpaly, P. Schwerdtfeger, H. Preuss, *J. Phys. B* **1983**, *16*, L323.
[28] P. Gray, T. C. Waddington, *Trans. Faraday Soc.* **1957**, *53*, 901.
[29] H. A. Papazian, *J. Chem. Phys.* **1961**, *34*, 1614.
[30] E. B. Wilson, J. C. Decius, P. C. Cross, *Molecular Vibrations*, McGraw-Hill, New York, **1955**.
[31] See, for example: a) I. R. Beattie, J. S. Ogden, R. S. Wyatt, *J. Chem. Soc. Dalton Trans.* **1983**, 219; b) E. G. Hope, P. J. Jones, W. Levason, J. S. Ogden, M. Tajik, J. W. Turff, *J. Chem. Soc. Dalton Trans.* **1985**, 529.

Received: September 6, 2005
Published online: February 21, 2006

